RevMexAA (Serie de Conferencias), **13**, 36–42 (2002)

H_2 OBSERVATIONS OF OUTFLOWS FROM YOUNG STARS

Christopher J. Davis

Joint Astronomy Centre, Hilo, Hawaii, USA.

RESUMEN

Analizamos observaciones del IR cercano recientes de jets Herbig-Haro (HH) y de flujos moleculares de protoestrellas muy jóvenes profundamente embebidas. Mediciones de movimiento propio y estudios espectroscópicos de baja y de alta resolución muestran la excitación y la cinemática de objetos individuales, que podrían interpretarse en términos de choques de proa de alta velocidad que barren y incorporan material del ambiente para formar flujos moleculares de "CO". Las propiedades observadas de muchos objetos puede explicarse razonablemente bien con modelos de choques de proa tipo "C" magnetizados, aunque choques del tipo "J" no puede excluirse del todo. Analizamos también nuevas observaciones echelle de las fuentes mismas de los flujos. Estos datos de H_2 muestran emisión de línea de velocidades intermedias y altas en la base del flujo (de menos de unas pocos cientos de unidades astronómicas de la fuente que lo impulsa) en la mayoría de las fuentes observadas. Las propiedades de estas regiones de líneas de emisión de hidrógeno molecular—o MHEL, por sus siglas en inglés—son similares a las regiones de líneas prohibidas (FEL, por sus siglas en inglés) hacia estrellas T Tauri.

ABSTRACT

Recent near-IR observations of Herbig-Haro (HH) jets and molecular outflows from very young, deeply embedded protostars are discussed. Proper motion measurements, and both low- and high-resolution spectroscopic studies reveal the excitation and kinematics of individual objects, which may be interpreted in terms of high-velocity bow shocks which sweep up and entrain ambient material to form molecular "CO" outflows. The observed properties of many objects can be explained reasonably well with magnetized bow C-shock models, although J-type shocks cannot be ruled out. We also discuss new echelle observations of the outflow sources themselves. These H_2 data reveal intermediate and high-velocity line emission from the base of the outflow (from within a few hundred AU of the driving source) in most of the flows observed. The properties of these "Molecular Hydrogen Emission Line"—or MHEL—regions, are similar to those of Forbidden Emission Line (FEL) regions towards T Tauri stars.

Key Words: **ISM: HERBIG-HARO OBJECTS — ISM: JETS AND OUTFLOWS — ISM: MOLECULAR HYDROGEN — STARS: PRE-MAIN-SEQUENCE**

Emission Lines from Jet Flows (Isla Mujeres, Q.R., México, November 13-17, 2000)
Editors: W. J. Henney, W. Steffen, A. C. Raga, & L. Binette

1. INTRODUCTION

We have witnessed in the last five years a rapid improvement in our ability to observe molecular outflows and Herbig-Haro (HH) jets at near-IR wavelengths. As a consequence, our understanding of the excitation and kinematics of individual objects, and the relationship between collimated jets, bow shocks and entrained ambient molecular gas has radically improved. Indeed, we are now able to observe and analyse Herbig-Haro-like shock features in outflows from some of the youngest and most heavily obscured protostars known.

High-resolution images of well-known HH objects in the $v = 1$–0, $J = 3$–1 transition of molecular hydrogen (the 1–0 $S(1)$ line) indicate a propensity for curved "bow shock" structures. Typically the H_2 traces the low-excitation molecular gas excited in the oblique wings of bow shocks, with higher-excitation optical and near-IR forbidden lines being excited nearer the cap of each bow (e.g., Figure 1). The bows themselves are driven by unseen, collimated jets. Cooling instabilities and flow variability probably cause the fragmented structure seen in many HH bow shocks.

2. H_2 BOWS AND CO OUTFLOWS: A CAUSAL RELATIONSHIP

There is growing support for the idea that much of the observed "intermediate-velocity" molecular gas (the traditional "CO" outflow; Bachiller 1996) in bipolar outflows is swept up predominantly by molecular bow shocks, the shocks themselves being driven by high-velocity collimated jets or winds.

Emission Lines from Jet Flows (Isla Mujeres, Q.R., México, November 13-17, 2000)
Editors: W. J. Henney, W. Steffen, A. C. Raga, & L. Binette

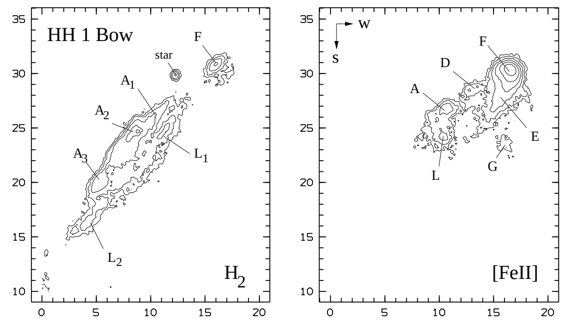

Fig. 1. H_2 and [Fe II] images of HH 1. The emission knots are all moving north-westward at a few hundred km s^{-1}. The H_2 is excited in the extended, almost planar shocks associated with the north-eastern edge of the overall structure; the [Fe II] is instead excited near the leading edge of HH 1.

These bows represent the jet-cloud interaction zone, and so are associated with current entrainment activity. The cooling time associated with H_2 in these shocks is very short, of the order of only a few years. Specifically, $t_c \sim 3 \times 10^8 n_6^{-1} T_3^{-2.3}$ for H_2 densities $n_6 = n/(10^6 \text{ cm}^{-3}) < 3$, where t_c is in seconds and T_3 is the temperature in units of 1000 K (Smith & Brand 1990). Once a jet exits the denser regions of the parental cloud, any associated bow shocks will fade rapidly. However, while still within the cloud, H_2 excitation and ambient gas entrainment will occur.

H_2 images of CO outflows testify to this entrainment process (Davis & Eislöffel 1995). Comparison of H_2 images of molecular bows with recent, high-resolution CO maps of outflows reveal compelling evidence for a causal relationship. The BIMA data of Lee et al. (2000) are particularly insightful (Figure 2), as are published CO and H_2 observations of the high-mass star-forming region W 75N. Note the close correlation between peaks in the CO and H_2 emission in HH 240 (Fig. 2). Similarly, in W 75N the extensive H_2 bow observed to the south-west of the source is seen to envelope the outer, leading edge of the blue-shifted CO outflow lobe (Davis et al. 1998), as one would expect if the lobe represents ambient gas swept up by the H_2 bow shock.

Analytical and numerical simulations of jet-driven flows reproduce with some degree of success the observed characteristics of the bow shocks and CO outflow lobes in W 75N, L 1634 and other regions (Raga & Cabrit 1993; Smith, Suttner, & Yorke 1997; Völker et al. 1999; Downes & Ray 1999; Lee et al. 2000). The models reproduce most of the observed morphological features, such as the bulge and limb-brightening seen in these and other CO outflows, although the model H_2 bows of Smith et al. tend to exhibit more structure along the flow axis: in W 75N, L 1634, and in many other flows the H_2 emission is usually confined to a thin hemispherical cap with a radius of curvature many times greater than the shock thickness or post-shock cooling length. These jet-driven outflow models also go some way towards explaining observed position-velocity plots, and the slope of the mass-velocity distribution, γ, usually measured across CO outflows (γ is quantified via a simple power-law of the form $m_v \propto v^{-\gamma}$), although opacity at low outflow velocities may effect many of the values reported in the literature (Yu et al. 2000). Also, γ will clearly change along the lobes of each outflow. One would expect the slope of the mass-velocity distribution, and so the value of γ, to *decrease* just behind an advancing shock front and towards the ends of the flow lobes, i.e., at locations in the flow where the ratio of low- to high-velocity gas will be reduced. This does indeed seem to be the case in, for example, the CO $J = 4$–3 map of V380 Ori NE (Davis et al. 2000).

3. H_2 EXCITATION ACROSS HH BOWS

Low- and intermediate-resolution near-IR spectroscopy of HH objects and H_2 bow shocks yields useful information about the gas excitation conditions. Although initial studies of a few well-known HH objects suggested a mostly thermal, single-temperature population distribution for H_2 levels with $v \leq 3$, a range of excitation temperatures have since been identified in some sources (Schwartz et al. 1995; Everett, DePoy, & Pogge 1995). There may also be a fluorescent contribution to the emission from higher-excitation H_2 lines, due to Lyα pumping of low-density, pre-shock gas (Fernandes & Brand 1995).

To better understand the physics of molecular bow shocks, we need to examine *changes* in excitation across individual shock fronts, as well as along the axes of HH jets and H_2 flows. To this end, we have conducted a detailed study of two molecular bow shocks in two separate outflows, HH 99 and VLA 1623A (HH 313) (Davis et al. 1999). High-resolution H_2 images reveal the well-defined bow shock morphologies of both sources. These we compare to the 2-D magnetohydrodynamic (MHD) models developed by Smith and co-workers (Smith & Brand 1990; Smith 1991; Yu et al. 2000). From the comparison we infer flow inclination angles, shock speeds and the magnetic field in the pre-shock gas in each bow. The same models are then compared

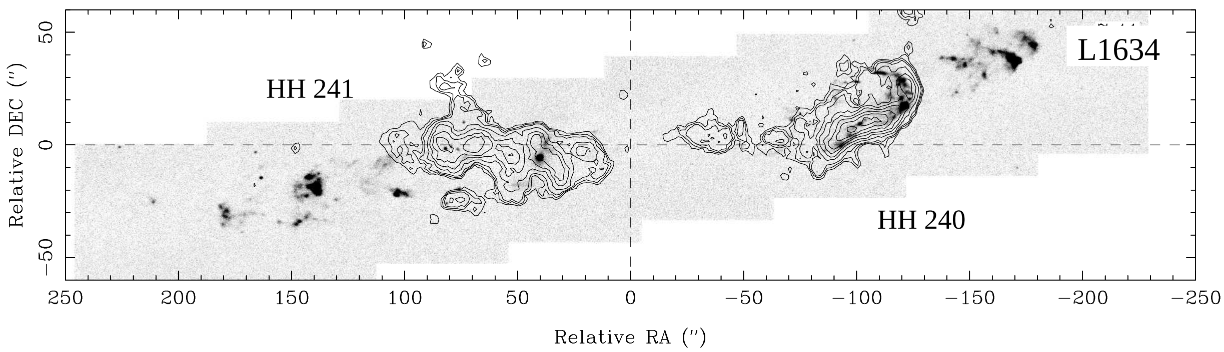

Fig. 2. H_2 1–0 $S(1)$ image of L 1634 (HH 240/241) with, superimposed, contours of CO 1–0 emission obtained with the BIMA array (from Lee et al. 2000).

Emission Lines from Jet Flows (Isla Mujeres, Q.R., México, November 13-17, 2000)
Editors: W. J. Henney, W. Steffen, A. C. Raga, & L. Binette

to excitation data. Towards the brighter target, VLA 1623A, we were able to extract spectra at four locations across the bow shock (the slit being orientated along the jet axis). A sample spectrum is shown here in Figure 3.

From the many H_2 ro-vibrational lines in the near-IR bands one can measure column densities for the upper energy levels and then plot *Column Density Ratio*, or CDR diagrams. A CDR plot clearly illustrates departures from single-temperature thermal excitation (which would result in all the points laying on a straight line, the slope of the line being a measure of the excitation temperature). CDR diagrams are described in detail by Burton & Haas (1997) and Eislöffel, Smith & Davis (2000).

Extinction-corrected column densities, derived from three of the four spectra observed across VLA 1623A, are plotted in Figure 4. Superimposed are model CDR curves, predicted by the same bow model used to synthesize the morphological features observed in the H_2 image of VLA 1623A. Kinematic information from the model was also compared to H_2 line profiles observed across the bow surface (see Davis et al. 1999 for details). For the first time, morphology, excitation *and* kinematics are fit with a single bow-shock model. Although only partially successful, we were able to predict (i) the decreasing excitation towards the bow flanks in VLA 1623A (Fig. 4), (ii) intensity distributions that compare very favorably with the high-resolution images of both targets, and (iii) narrow, low-velocity H_2 line profiles similar to those observed.

In a similar study, we (Eislöffel et al. 2000) later examined excitation and kinematic information extracted from intermediate resolution spectra at a number of locations across a further five outflows. As with our earlier study, we found that the data support a picture in which excitation variations are caused by large-scale shock geometries. The variations are best interpreted with MHD C-shocks, although some locations which demonstrate hydrodynamic J-type excitation were also found. In two targets, the jets themselves were also traced in H_2 emission. We find that the excitation declines with distance from each source. Tedds et al. (these proceedings) likewise discuss changing excitation—from knot to knot—along the axes of three collimated jets, HH 212, HH 111 and HH 46.

4. KINEMATICS OF H_2 BOW SHOCKS

After repeated H_2 imaging campaigns, some groups have taken a first stab at measuring the proper motions of H_2 features in a few outflows. Typically, the tangential velocities match those of optical studies of the same HH objects. This clearly indicates that the H_2 and optical forbidden line emissions derive from the same shock features. However, in some outflows H_2 is excited in different parts of the flow, or in the optically-obscured counterflow. Thus, near-IR proper motion measurements can be complementary to optical kinematic studies.

In HH 46/47, for example, the inferred tangential velocities range from a few tens to almost 500 km s^{-1} (Micono et al. 1998). The highest velocities are observed for H_2 knots either in or close to the jet/counterjet axis. Knots constituting the wings of the large scale H_2 bow seen in the counterflow are found to move much more slowly. In HH 111 and HH 121 (see Figure 5) tangential velocities in the range 265–460 km s^{-1} are measured (Coppin, Davis, & Micono 1998), while in HH 1 speeds of 150–400 km s^{-1} are recorded (Noriega-Crespo et al. 1997). In almost all cases, the tangential velocities exceed the dissociation speed limit for molecular hydrogen in shocks in dense gas; this indicates that the

Emission Lines from Jet Flows (Isla Mujeres, Q.R., México, November 13-17, 2000)
Editors: W. J. Henney, W. Steffen, A. C. Raga, & L. Binette

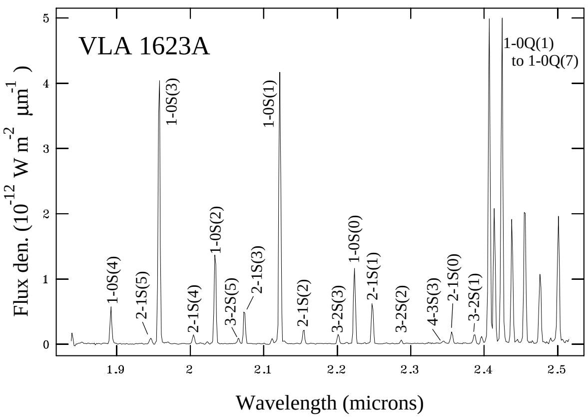

Fig. 3. One of three K-band spectra obtained in the HH bow shock VLA 1623A (HH 313).

associated shock velocities are much lower than the shock pattern speeds (the proper motions) and the underlying jet speeds.

Variability of H_2 features were also noted in some outflows. In HH 111 and HH 46/47 several knots significantly changed their luminosity and/or morphology over the 4–5 year timebase used to conduct each study. From these changes a molecular cooling time of the order of a few years is thus inferred, in line with theoretical predictions based on "typical" jet densities and velocities (as noted earlier). More recent proper motion studies for HH 7–11, HH 33/40 and HH 25/26 are discussed by Chrysostomou et al. elsewhere in these proceedings (see also Chrysostomou et al. 2000).

By comparison, H_2 radial velocity measurements are far more common-place (e.g., Carr 1993; Davis & Smith 1996a, 1996b; Tedds et al. 1999; Yu et al. 2000). Typically, H_2 emission lines in HH objects are blue or red shifted by a few tens of km s^{-1} from the systemic velocity. Line widths are usually $\sim$ 50 km s^{-1} FWHM (although broader lines are evident in the nearby high-mass star forming region OMC-1, Tedds et al. 1999). Lines are often single-peaked and roughly Gaussian in shape, although double-peaked and asymmetric profiles have been observed. In a few H_2 bow shocks double-peaked profiles are detected in the bow flanks. In HH 7, for example, the velocity separation between the low and high-velocity blue-shifted peaks is of the order of 70 km s^{-1}, whereas in the HH 72B and L 1551-IRS 5 bow shocks we observe a peak-to-peak separation that is considerably larger, approaching 150 km s^{-1}(Davis et al. 2001). Double-peaked profiles are expected in hollow, shell-like bow shocks,

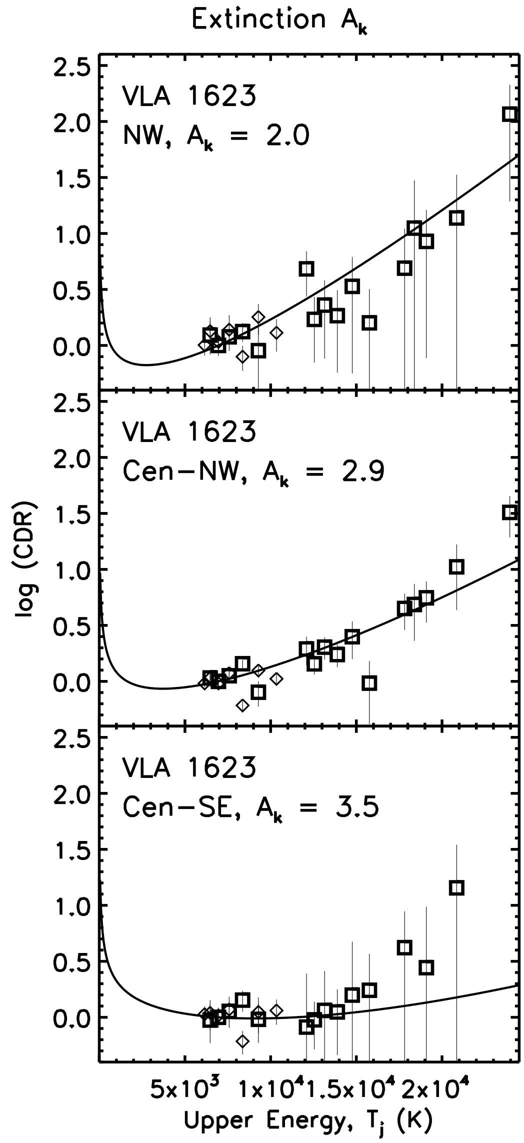

Fig. 4. Comparison of model CDR curves to (extinction-corrected) H_2 column densities derived from spectra obtained at three positions across VLA 1623A. Only the K-band data are used. Data at locations near the bow head (top), near the bow center (middle) and towards the bow flanks (bottom) are plotted. The solid lines are CDR curves predicted by the same model used to synthesize the observed morphology and luminosity of the bow shock; they are *not* fits to the data. The same MHD models are also used to predict H_2 profiles, for comparison with H_2 echelle observations. See Davis et al. (1999) for details.

where emission is excited in the near and far sides of the bow shock shell. In these three examples, the

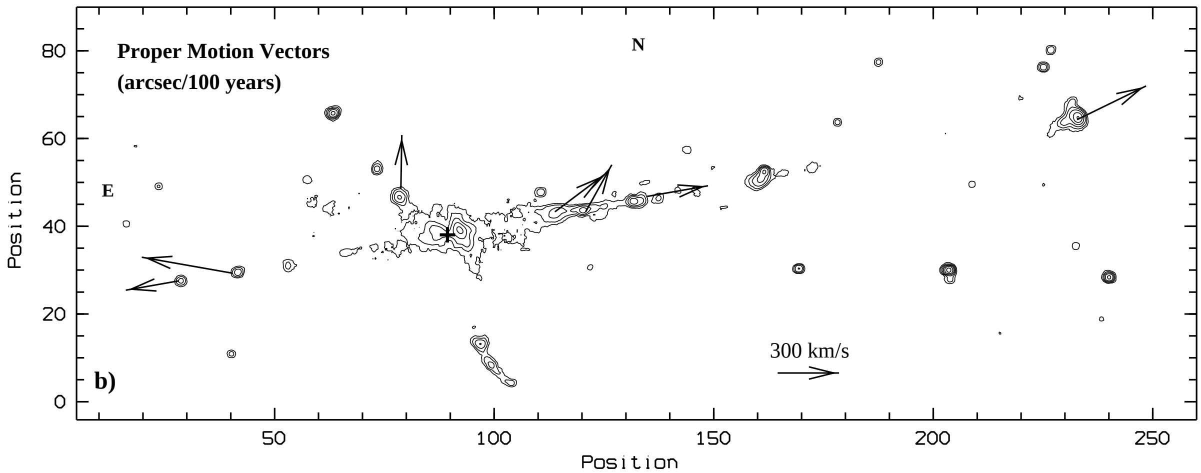

Fig. 5. Proper motions of H_2 knots in HH 111 and HH 121 (Coppin et al. 1998).

low-velocity component is brighter than the high-velocity peak, which would be consistent with a high-velocity "bullet" interpretation, rather than a "shocked stationary clump" model (e.g., Hartigan et al. 1987). However, the peak-to-peak separations, and the overall velocity extent of the emission lines, are remarkably high.

Models of line profiles from unresolved bow shocks predict that the Full-Width at Zero Intensity (FWZI) extent of the lines should be equivalent to the overall bow shock velocity (Hartigan et al. 1987). However, this analytical treatment assumes that emission comes from all parts of the bow shock. In fast molecular bows H_2 will be dissociated near the head of the bow, where shock speeds (normal to the shock surface) exceed the molecular dissociation "speed limit", $v_{\rm d}$, which is of the order of $\sim$ 50 km s^{-1} in magnetic C-shocks, unless the magnetic field is extremely high (Smith 1994) or the preshock density low. The maximum velocity dispersion from a planar shock is therefore limited to $v_{\rm d}$. If the flow is orientated close to the plane of the sky, then the *maximum* FWZI velocity dispersion measurable in H_2 from a bow is given by $\Delta V_{\rm FWZI} = 2v_{\rm d} \sin\theta \cos\alpha_{\rm d}$, where θ is the orientation angle of the flow with respect to the line of sight and $\alpha_{\rm d} = \sin^{-1}(v_{\rm d}/v_{\rm s})$ is the maximum angle between the shock plane and the bow shock direction for which H_2 survives to be excited, in which $v_{\rm s}$ is the bow shock velocity along the flow axis.[1]

[1]Note that this may be different from the velocity of the bow with respect to the "stationary" source, since the knots in a jet may be internal shocks that impact moving jet gas ahead of them.

The quantity $\Delta V_{\rm FWZI}$ is strongly dependent on $v_{\rm d}$; indeed, the FWZI velocity dispersion should never exceed $2v_{\rm d} \sim 100$ km s^{-1}. This does seem to be the case in many outflows, though not in all. For example, the double-peaked profiles noted earlier (in HH 72B and L 1551-IRS5) are somewhat broader. The overall profile shapes may therefore not simply be the result of bow shock geometry. Instead, the low and high-velocity components may represent emission from bow shock gas and jet material, respectively. The low-velocity component could be radiating from precursor gas just ahead of an advancing C-type bow shock; this would explain the low peak velocity and broad line profiles. The high-velocity gas could then be excited in the jet flow, perhaps in the Mach disk, although this would require a molecular component to the underlying jet. Note that we do see the low-velocity component extending further ahead (downwind) of the high-velocity H_2—at least in the three examples considered here—which would be expected of such a scenario.

5. H_2 EMISSION FROM THE BASE OF YSO JETS—"MHEL" REGIONS REVEALED.

In addition to the high-velocity H_2 observed in the extended lobes of HH jets and molecular outflows (discussed in the previous section), H_2 has also been detected towards a number of outflow sources (Greene & Lada 1996; Reipurth & Aspin 1997). We have recently examined the properties of these emission regions via echelle spectroscopy observations of nine outflow sources (Davis et al. 2001). H_2 and Brγ observations were obtained towards each Class I source, with the spectrometer slit orientated along

Emission Lines from Jet Flows (Isla Mujeres, Q.R., México, November 13-17, 2000)
Editors: W. J. Henney, W. Steffen, A. C. Raga, & L. Binette

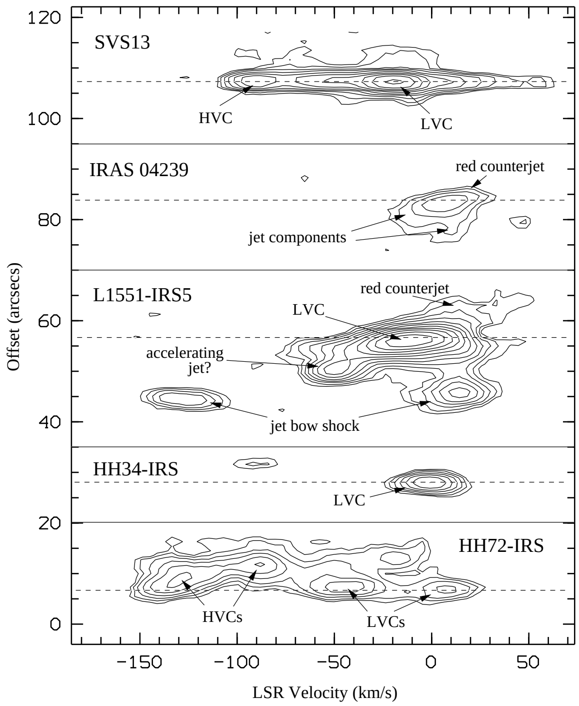

Fig. 6. H_2 Position-Velocity plots towards Class I HH energy sources. The continuum emission from each source (marked with a dashed line) has been removed to leave only the line emission associated with each MHEL region.

the flow axis in each case. Brγ and/or H_2 was detected towards most of the sources. However, we found a number of distinct differences between the H_2 and Brγ results. The Brγ profiles are much wider than their H_2 counterparts, although the H_2 profiles are, in a few cases at least, more structured (less Gaussian). Also, in all cases the Brγ emission is confined to the outflow source, being unresolved along the slit/outflow direction, whereas the H_2 is extended along the flow axis, even towards sources where H_2 is detected only towards the source position.

To better illustrate the extended H_2 regions we plot in Figure 6 contour diagrams of five outflow source regions. The continuum emission associated with each YSO has been fitted and removed, row-by-row via linear least-squares fits to the emission on either side of the H_2 line-emission peaks, so that only the line emission remains. Multiple velocity components are revealed in most sources (described in detail by Davis et al. 2001). Also, from Gaussian fits to the H_2 emission peaks and continuum strips either side of the H_2 regions we were able to measure the spatial offsets of the H_2 components from the continuum position. In four of the five sources shown here we found clear offsets of the H_2 emission, by a few tenths of an arcsecond, from the driving YSO (there was no measurable offset in HH 34-IRS). Moreover, in individual objects, the offset was found to increase at higher blue-shifted velocities.

H I profiles have been observed in a large number of classical T Tauri stars (e.g., Hartmann, Hewett & Calvet 1994; Folha & Emerson 2001). Line shapes are typically interpreted in terms of magnetospheric accretion (Muzerolle, Calvet, & Hartmann 1998), although the profiles may also be modified by outflow processes. The Brγ profiles observed towards the Class I sources in our survey are probably produced in the same way. The H_2 emission is, on the other hand, almost certainly associated with the outflow in each system, since it is extended along the outflow axis and in most cases offset from the outflow position (by a few tenths of an arcsecond, or a few hundred AU). Indeed, the properties of these H_2 line emission regions, observed in our sample of Class I outflow sources, are very similar to those of *Forbidden Emission-Line* (FEL) regions observed in many classical T Tauri stars (Hartigan, Edwards, & Ghandour 1995; Hirth, Mundt, & Solf 1997). Consequently, we refer to these regions as *Molecular Hydrogen Emission Line*, or MHEL, regions.

A number of theories have been presented to explain the FEL regions observed in TTSs (e.g., Kwan & Tademaru 1995; Ouyed & Pudritz 1994). These models may also explain the MHEL regions observed towards the younger, Class I outflow sources. For FELs, a model that assumes two independent flow components is preferred (Hirth et al. 1997), since this accounts for the different excitation conditions observed in low and high-velocity components in FELs. Kwan (1997) suggests that while the high-velocity component (HVC) probably derives from a collimated, high-velocity jet, the low-velocity component (LVC) could be produced in a warm disk corona or a slow disk wind.

Typically the MHEL line profile widths measure 60–160 km s^{-1} (FWZI). Such line broadening could be due to Keplerian rotation in or near the accretion disk surface (Hartigan et al. 1995), or simply through lateral expansion of the outflowing gas (Hamann 1994). If the former applies, then the FWZI of each H_2 profile should reflect the maximum velocity attained in the inner regions of the accretion disk. Given the inclination angle of the flow to the line of sight, θ, one may estimate the maximum Keplerian velocity associated with the H_2 and Brγ emission regions, since $V_{\rm kep} = \Delta V_{\rm FWZI}/(2\sin\theta)$. The narrow H_2 profiles obviously lead to a much lower velocity than the Brγ observations. Since $V_{\rm kep}^2$ is inversely related to the radial distance of the emitting "ring", it is not surprising that the higher-excitation Brγ emission would derive from much closer in to the star. Indeed, for a $1\,M_\odot$ star, a typical broadened Brγ profile with $V_{\rm kep} \sim 250$ km s^{-1} could originate from a ring of radius $\sim 2\times10^{11}$ cm; the H_2 would then arise from further out in the disk plane, at a radius of $\sim 9\times10^{12}$ cm for a Keplerian velocity of 40 km s^{-1}.

Since the MHEL regions are almost certainly associated with each outflow, the H_2 profiles could instead be broadened by expansion of the flow lobe. Taking into account the inclination angle of the flow axis, θ, the flow opening angle, $\alpha = 2.0\arctan(\Delta V_{\rm FWZI}\cos\theta/2V_{\rm peak})$, where $V_{\rm peak}$ is the velocity of the HVC or LVC emission peak. For "typical" values of $\Delta V_{\rm FWZI} \sim 70$ km s^{-1} and $\theta \sim 45°$ the full opening angle of an LVC with $V_{\rm peak} \sim 20$ km s^{-1} would be roughly 100°; by comparison, an HVC with a similar FWZI though a $V_{\rm peak} \sim 70$ km s^{-1} would have an opening angle of the order of 40°. These very crude values are likely to be overestimated, since turbulence and thermal motions will contribute to the line broadening. The observations, particularly of SVS 13 where both LVC and HVC components are detected in H_2 (Fig. 6), do nevertheless indicate that the HVC is probably more highly collimated than the LVC, as is the case with optical FEL regions.

REFERENCES

Bachiller, R. 1996, ARA&A, 34, 111
Burton, M. G., & Haas, M. R. 1997, A&A, 327, 309
Carr, J. S. 1993, ApJ, 406, 553
Chrysostomou, A., Hobson, J., Davis, C. J., Smith, M. D., & Berndsen, A., 2000, MNRAS, 314, 229
Coppin, K. E. K., Davis, C. J., & Micono, M. 1998, MNRAS, 301, L10
Davis, C. J., Dent, W. R. F., Matthews, H. E., Coulson, I. M., & McCaughrean M. J. 2000, MNRAS 318, 952
Davis, C. J., & Eislöffel, J. 1995, A&A, 300, 851 (Erratum: A&A, 305, 694)
Davis, C. J., Ray, T. P., Desroches, L., & Aspin, C. 2001, MNRAS, 326, 524
Davis, C. J., & Smith, M. D. 1996a, A&A, 309, 929
———. 1996b, A&A, 310, 961
Davis, C. J., Smith, M. D., Eislöffel, J., & Davies, J. K. 1999, MNRAS, 308, 539
Davis, C. J., Smith, M. D., & Moriarty-Schieven, G. H. 1998, MNRAS, 299, 825
Downes, T. P., & Ray, T. P. 1999, A&A, 345, 977
Eislöffel, J., Smith, M. D, & Davis, C. J. 2000, A&A, 359, 1147
Everett, M. E., DePoy, D. L., & Pogge, R. W. 1995, AJ, 110, 1295
Fernandes, A. J. L., & Brand, P. W. J. L. 1995, MNRAS, 274, 639
Folha, D. F. M. & Emerson, J. P. 2001, A&A, 365, 90
Greene, T. P., & Lada, C. J. 1996, AJ, 112, 2184
Hamann, F. 1994, ApJS, 93, 485
Hartigan, P., Edwards, S., & Ghandour, L. 1995, ApJ 452, 736
Hartigan, P., Raymond, J. C., & Hartmann, L. 1987, ApJ, 316, 323
Hartmann, L., Hewett, R., & Calvet, S. 1994, ApJ, 426, 669
Hirth, G., Mundt, R., & Solf, J. 1997, A&AS, 126, 437
Kwan, J. 1997, ApJ, 489, 284
Kwan, J, & Tademaru, E. 1995, ApJ, 454, 382
Lee, C. F., Mundy, L. G., Reipurth, B., Ostriker, E. C., & Stone, J. M. 2000, ApJ, 542, 925
Micono, M., Davis, C. J., Ray, T. P., Eislöffel, J., & Shetrone, M. D. 1998, ApJ, 494, L227
Muzerolle, J., Calvet, N., & Hartmann, L. 1998a, ApJ, 116, 2965
Noriega-Crespo, A., Garnavich, P. M., Curiel, S., Raga, A. C., & Ayala, S. 1997, ApJ, 486, L55
Ouyed, R., & Pudritz, R. E. 1994, ApJ, 423, 753
Raga, A. C., & Cabrit, S. 1993, A&A, 278, 267
Reipurth, B., & Aspin, C. 1997, AJ, 114, 2700
Schwartz, R. D., Schultz, A. S. B., Cohen, M., & Williams, P. M. 1995, ApJ, 446, 318
Smith, M. D. 1991, MNRAS, 252, 378
Smith, M. D. & Brand, P. W. J. L. 1990, MNRAS, 243, 498
———. 1994, MNRAS, 266, 238
Smith, M. D., Suttner, G., & Yorke, H. W. 1997a, A&A, 323, 223
Tedds, J. A., Brand, P. W. J. L., & Burton, M. G. 1999, MNRAS, 307, 337
Völker, R., Smith, M. D., Suttner, G., & Yorke, H. W. 1999, A&A, 343, 953
Yu, K. C., Billawala, Y., Smith, M. D., Bally, J., & Butner, H. M. 2000, AJ, 120, 1974

C. J. Davis, Joint Astronomy Centre, 660 North A'ohōkū Place, University Park, Hilo, Hawaii 96720, USA (c.davis@jach.hawaii.edu).

Emission Lines from Jet Flows (Isla Mujeres, Q.R., México, November 13-17, 2000)
Editors: W. J. Henney, W. Steffen, A. C. Raga, & L. Binette